Spherical Collapse and Galaxy Clusters

Marcos Lima

2018

Outline

- Closed Universe: Expansion and Collapse
- Spherical Collapse
- Cluster Mass-function
- Cluster Counts
- Cluster Bias
- Cluster Covariance
- Cluster Likelihood
- Cluster Forecasts
- Cluster Constraints

Closed Universe

- FRW metric (background) with positive curvature ($k > 0$):

$$ds^2 = -dt^2 + a^2(t)\left[\frac{dr^2}{1 - kr^2} + r^2 d\theta^2 + r^2 \sin^2\theta d\phi^2\right]$$

- Friedmann equations (matter only):

$$\begin{aligned} \left(\frac{\dot{a}}{a}\right)^2 &= \frac{8\pi G\bar{\rho}_m}{3} - \frac{k}{a^2} \\ \frac{\ddot{a}}{a} &= -\frac{4\pi G}{3}\bar{\rho}_m \end{aligned}$$

Closed Universe

- FRW metric (perturbations):

$$ds^2 = -(1-2\Psi)dt^2 + a^2(t)(1+2\Psi)\left[\frac{dr^2}{1-kr^2} + r^2 d\theta^2 + r^2 \sin^2\theta d\phi^2\right]$$

- Poisson equation:

$$\nabla^2\Psi = 4\pi G a^2 \delta\rho_m$$

where $\delta\rho_m = \rho_m - \bar{\rho}_m$

Newtonian Interpretation

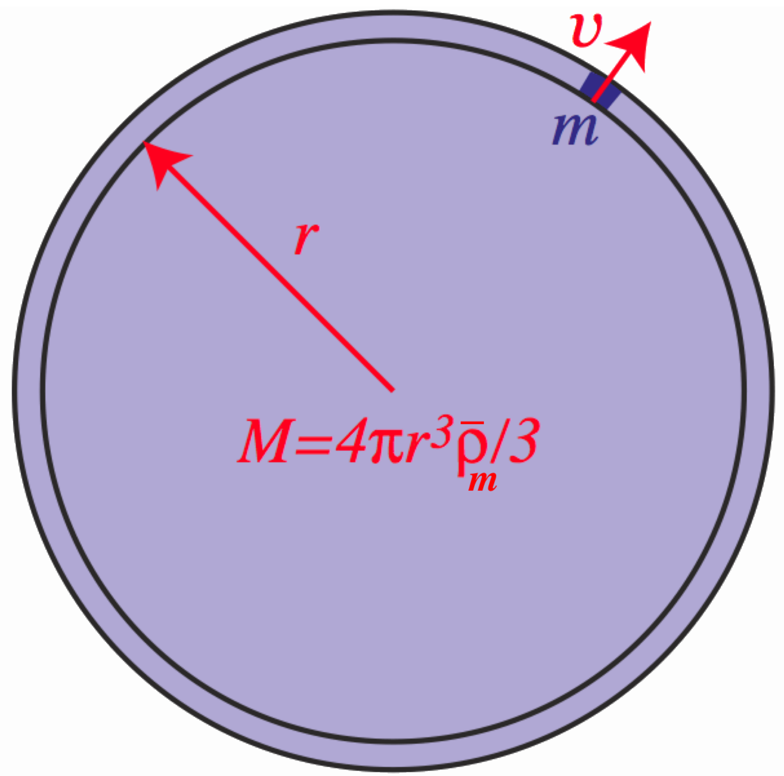

W. Hu

- Energy of test particle m:

$$E = \frac{1}{2}mv^2 - \frac{GMm}{r} = \text{const.}$$

$$\rightarrow \left(\frac{\dot{r}}{r}\right)^2 = \frac{8\pi G}{3}\bar{\rho}_m + \frac{\text{const.}}{r^2}$$

- Closed universe: $\text{const} < 0$ represents curvature. Gravitational potential energy wins over kinetic energy.
- Precise value of const given in GR.

Newtonian Interpretation

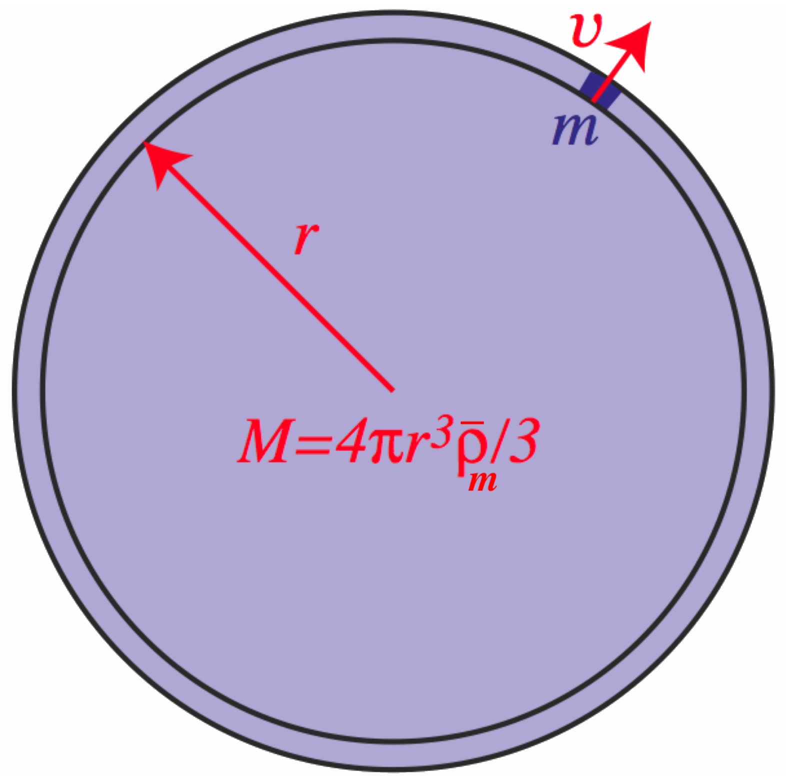

- Force on test particle m:

$$
\begin{aligned}
F &= m\frac{d^2r}{dt^2} = -\frac{GMm}{r^2} \\
\rightarrow \frac{\ddot{r}}{r} &= -\frac{4\pi G}{3}\bar{\rho}_m
\end{aligned}
$$

- Acceleration equation does not involve curvature.
- Should be true also for spherical top-hat perturbations !

W. Hu

Spherical Collapse

- Idealized model: qualitative features of cluster formation.
- Homogeneous top-hat spherical perturbation within a homogeneous background.
- Perturbation expands, reachs a maximum radius (turns around) and collapses (virializes).
- Initial top-hat remains a top-hat during evolution.
- Cluster expands and collapses as a separate closed universe: Birkhoff theorem in GR.
- Allows analytical (numerical) computation of linear overdensity at collapse δ_c and overdensity at virialization Δ_{vir}, for interpretation in Press-Schechter theory.

Spherical Collapse: Newtonian

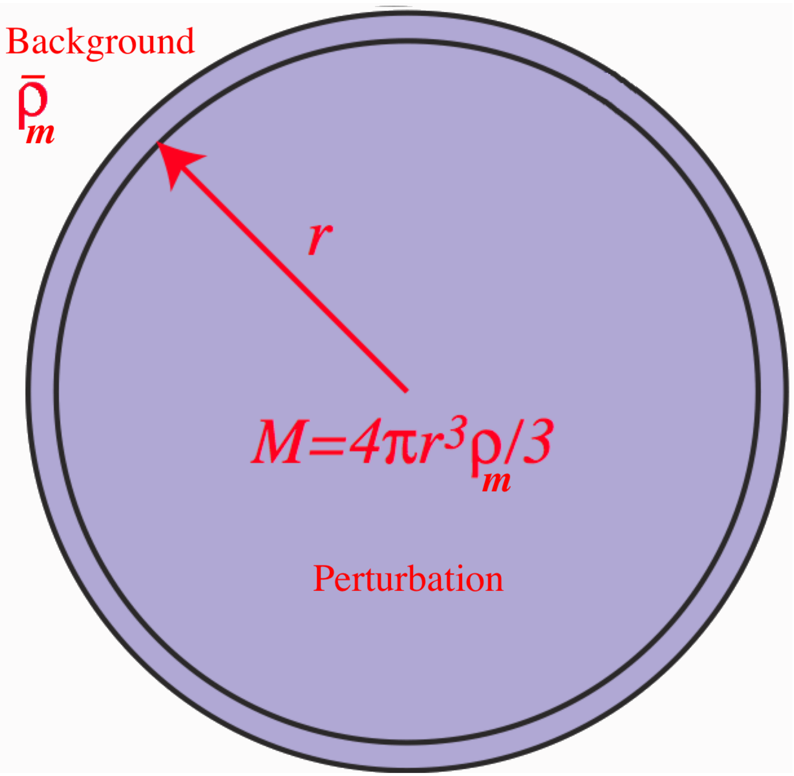

- Background (flat):

$$\left(\frac{\dot{a}}{a}\right)^2 = \frac{8\pi G}{3}\bar{\rho}_m$$

- Spherical top-hat perturbation (separate closed universe):

$$\frac{\ddot{r}}{r} = -\frac{4\pi G}{3}\rho_m$$

Spherical Collapse: Relativistic

- More generally, use GR and consider fluid equations:

$$\begin{aligned} \frac{\partial \delta}{\partial t} + \frac{1}{a}\nabla\cdot(1+\delta)\mathbf{v} &= 0\,, && \text{Continuity} \\ \frac{\partial \mathbf{v}}{\partial t} + \frac{1}{a}(\mathbf{v}\cdot\nabla)\mathbf{v} + H\mathbf{v} &= -\frac{1}{a}\nabla\Psi\,, && \text{Euler} \end{aligned}$$

where $\delta = \delta\rho_m/\bar{\rho}_m$. For a top-hat, $\mathbf{v} = A(t)\mathbf{r}$, so combine eqs.:

$$\frac{\partial^2 \delta}{\partial t^2} + 2H\frac{\partial \delta}{\partial t} - \frac{4}{3}\frac{\dot{\delta}^2}{(1+\delta)} = \frac{(1+\delta)}{a^2}\nabla^2\Psi\,, \qquad \text{Full}$$

- In linear theory $\delta = \delta_L \ll 1$ and

$$\frac{\partial^2 \delta_L}{\partial t^2} + 2H\frac{\partial \delta_L}{\partial t} = \frac{\nabla^2\Psi}{a^2}\,, \qquad \text{Linear}$$

Spherical Collapse

$$\ddot{\delta} + 2H\dot{\delta} - \frac{4}{3}\frac{\dot{\delta}^2}{(1+\delta)} = \frac{(1+\delta)}{a^2}\nabla^2\Psi\,, \qquad \text{Full}$$

- Mass conservation during collapse:

$$M = (4\pi/3)r^3\bar{\rho}_m(1+\delta) = \text{const.}$$

- Replace $\delta \to r$, and use $\nabla^2\Psi = 4\pi G a^2 \delta\rho_{\rm m}$:

$$\begin{aligned}\frac{\ddot{r}}{r} &= -\frac{4\pi G}{3}\bar{\rho}_m - \frac{\nabla^2\Psi}{3a^2} \\ &= -\frac{4\pi G}{3}\rho_m\end{aligned}$$

- Same result as Newtonian approach!

Spherical Collapse: Matter only

- Background + Spherical Perturbation:

$$\left(\frac{\dot{a}}{a}\right)^2 = \frac{8\pi G}{3}\bar{\rho}_m \quad \text{Background}$$

$$\frac{\ddot{r}}{r} = -\frac{4\pi G}{3}\rho_m \quad \text{Spherical Perturbation}$$

- Analytical solution for $a(t)$:

$$a(t) \propto t^{2/3}$$

- Parametric cyclic solution for $r(t)$:

$$\begin{aligned} r(\theta) &\propto 1 - \cos\theta \\ t(\theta) &\propto \theta - \sin\theta \end{aligned}$$

Linear collapse density contrast

- Beginning: $\theta = 0$.
- Turn-around: $\theta_{ta} = \pi$.
- Collapse: $\theta_c = 2\pi$.

- Since solution fully known, can compute exactly important quantities for the collapse.
- By definition $r = 0$ and $\delta = \infty$ at collapse a_c.
- But linear theory value extrapolated to a_c remains finite:

$$\delta_c = \delta_L(a_c) = \frac{3}{5}\left(\frac{3\pi}{4}\right)^{2/3} \approx 1.686$$

Virial overdensity

- In reality, perturbations not spherical, nor top-hat (profile)$\rightarrow$ Shell-crossing. Assume virialization happens before collapse. Virial equilibrium achieved when

$$U = -2K \quad \text{Virial Theorem}$$

- Energy conservation at turn-around (a_{ta}) and virialization (a_{vir})

$$E = U + K = U(a_{ta}) = \frac{1}{2}U(a_{vir})$$

- Top-hat sphere: $U = 3/5GM^2/r$, so $r_{vir} = r_{ta}/2 \rightarrow \theta_{vir} = 3\pi/2$.
- Overdensity at collapse (virialization):

$$\Delta_{vir} = \frac{\rho_m(a_{vir})}{\bar{\rho}_m(a_c)} = \frac{\rho_m(\theta = 3\pi/2)}{\bar{\rho}_m(\theta = 2\pi)} = 18\pi^2 \approx 178$$

Spherical Collapse: Matter + DE

- Matter + Dark Energy with constant w_{DE}:

$$\left(\frac{\dot{a}}{a}\right)^2 = \frac{8\pi G}{3}\left[\bar{\rho}_m + \bar{\rho}_{DE}\right] \quad \text{Background}$$

$$\frac{\ddot{r}}{r} = -\frac{4\pi G}{3}\left[\rho_m + \bar{\rho}_{DE}(1+3w_{DE})\right] \quad \text{Perturbation}$$

- Analytical solution for $a(t) \propto \sinh^{2/3}(Bt)$.
- No analytical or parametric solution for $r(t)$.

  Must be solved numerically to compute δ_c and Δ_{vir}.

ΛCDM: δ_c

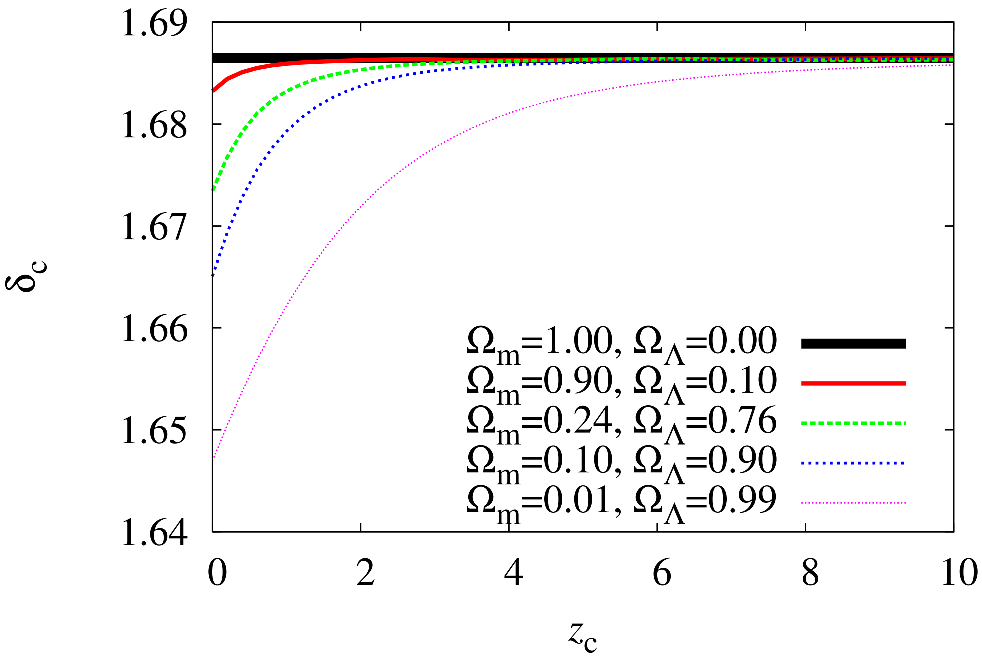

- Dark energy changes collapse time and linear growth.
- Small change in δ_c compared to matter-only Universe.
- Changes also in Δ_{vir}.

Halo Mass-Function: Press-Schechter

- Define $\sigma^2(M)$: variance of the linear density field smoothed on a scale R corresponding to mass M:

$$\sigma^2(M) = \frac{1}{(2\pi)^3} \int d^3k |\tilde{W}(kR)|^2 P_m^L(k) \, ,$$

  $P_m(k)$: Linear power spectrum and

  $\tilde{W}(kR)$: top-hat window of radius $R(M)$ with $M = \bar{\rho}_{\rm m} 4\pi R^3/3$.

- Initial density field approximately Gaussian:

$$P(\delta|M) = \frac{1}{\sqrt{2\pi}\sigma(M)} \exp\left[-\frac{\delta^2}{2\sigma^2(M)}\right]$$

- Peak density: $\nu^2 = \delta_c^2/\sigma^2$.

Halo Mass-Function: Press-Schechter

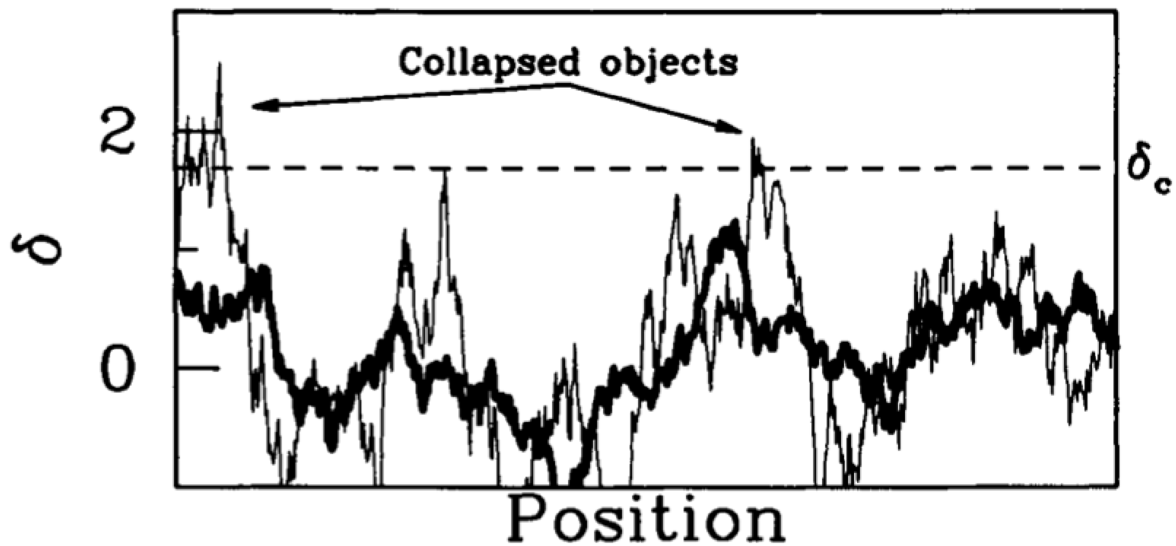

- Spherical collapse: dark matter regions with contrast $\delta > \delta_c$ evolve to form collapsed virialized halos.
- Fraction $F(> M)$ of matter that ends up in halos of mass $> M$:

$$F(> M) = \int_{\delta_c}^{\infty} d\delta P(\delta|M)$$

Halo Mass-Function: Press-Schechter

- Spherical collapse: dark matter regions with contrast $\delta > \delta_c$ evolve to form collapsed virialized halos.
- Fraction $F(> M)$ of matter that ends up in halos of mass $> M$:

$$F(> M) = \frac{1}{\sqrt{2\pi}\sigma(M)} \int_{\delta_c}^{\infty} d\delta \exp\left[-\frac{\delta^2}{2\sigma^2(M)}\right] = \frac{1}{2}\mathrm{erfc}\left[\frac{\nu^2}{\sqrt{2}}\right]$$

  where peak density: $\nu = \delta_c/\sigma$.

- Even when $\sigma(M) \to 0$, $F(> M) = 1/2$, i.e. only half of the dark matter is in halos.
- Integrating above δ_c, only overdense regions participate in the collapse. In reality, underdense regions also contribute.

Halo Mass-Function: Press-Schechter

- To compensate, multiply by an ad hoc factor or 2. Peacock 1999
- Differential fraction dF/dM of matter at halos in $[M, M+dM]$

$$\frac{dF}{dM} = 2\frac{dF}{d\nu}\frac{d\nu}{dM} = 2\frac{1}{\sqrt{2\pi\sigma^2}}\exp\left[-\frac{\delta_c^2}{2\sigma^2}\right]\left[-\delta_c\frac{d\sigma}{dM}\right]$$
$$= \sqrt{\frac{2}{\pi}}\frac{d\ln\sigma^{-1}}{dM}\,\nu\,\exp\left[-\frac{\nu^2}{2}\right]$$

- Matter number density $n_m = \bar{\rho}_m/M$
- Then the differential halo number density or mass-function:

$$\frac{dn}{d\ln M} = n_m\frac{dF}{d\ln M} = \sqrt{\frac{2}{\pi}}\frac{\bar{\rho}_{\rm m}}{M}\frac{d\ln\sigma^{-1}}{d\ln M}\nu\exp\left[-\frac{\nu^2}{2}\right]$$

Halo Mass-Function

- More generally, mass-function written as

$$\frac{dn(M,z)}{d\ln M} = f(\nu)\frac{\bar{\rho}_{\rm m}}{M}\frac{d\ln\sigma^{-1}}{d\ln M},$$

- Press-Schechter mass-function:

$$f(\nu) = f(\sigma,\delta_c) \quad = \quad \sqrt{\frac{2}{\pi}}\nu\exp\left[-\frac{\nu^2}{2}\right]$$ Press-Schechter

- Ellipsoidal collapse: improvement over the spherical model. One dimension collapses first, resulting ellipsoid becomes the halo. Based on this idea, Sheth and Tormen 99 proposed

$$f(\nu) \quad = \quad A[1+(a\nu^2)^{-p}]\sqrt{a\nu^2}\exp\left[-a\frac{\nu^2}{2}\right]$$ Sheth-Tormen

Halo Mass-Function

- Sheth-Tormen: $a = 0.75$ and $p = 0.3$ fit to N -body simulations.
- Press-Schechter: $a = 1$ and $p = 0$.
- Empirical fits to simulations improved mass-function accuracy beyond theoretical models. Drop δ_c dependence, so $f(\nu) = f(\sigma)$
- PS approach still motivates the general functional form of the fits. For instance, Jenkins et al 2001 provides a fit for spherical overdensity (SO) detected halos in ΛCDM:

$$f(\sigma) \quad = \quad 0.316 \exp(-|\ln \sigma^{-1} + 0.67|^{3.82}) \qquad \text{Jenkins}$$

- More recently, Tinker et al 2008 fits for a suite of high-resolution simulations and SO halos:

$$f(\sigma) \quad = \quad A \left[\left(\frac{\sigma}{b} \right)^{-a} + 1 \right] \exp \left[-\frac{c}{\sigma^2} \right] \qquad \text{Tinker}$$

Tinker Mass-Function

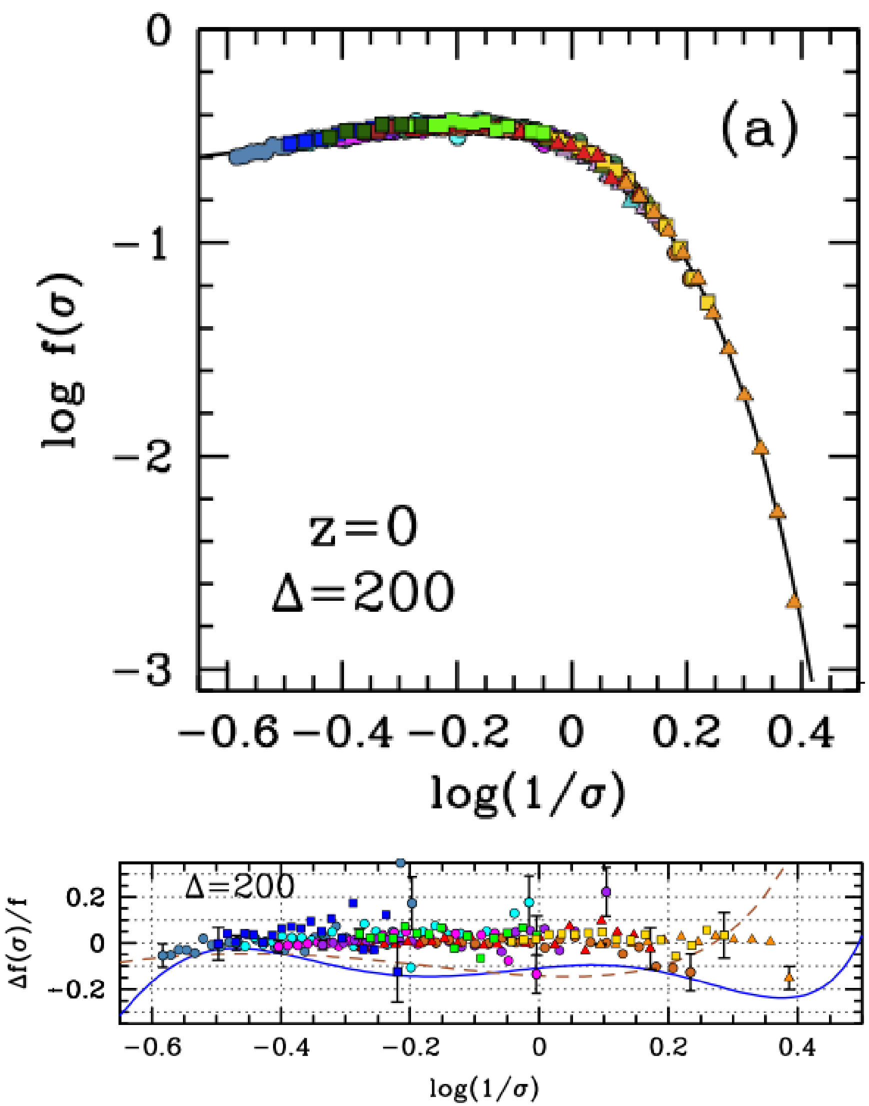

Tinker et al. 2008

- Tinker fits simulation results within $10 - 20\%$ accuracy.
- Sheth-Tormen (dashed) and Jenkins (blue) generally consistent as well, but less accurate.

$f(R)$ gravity: Halo-mass function

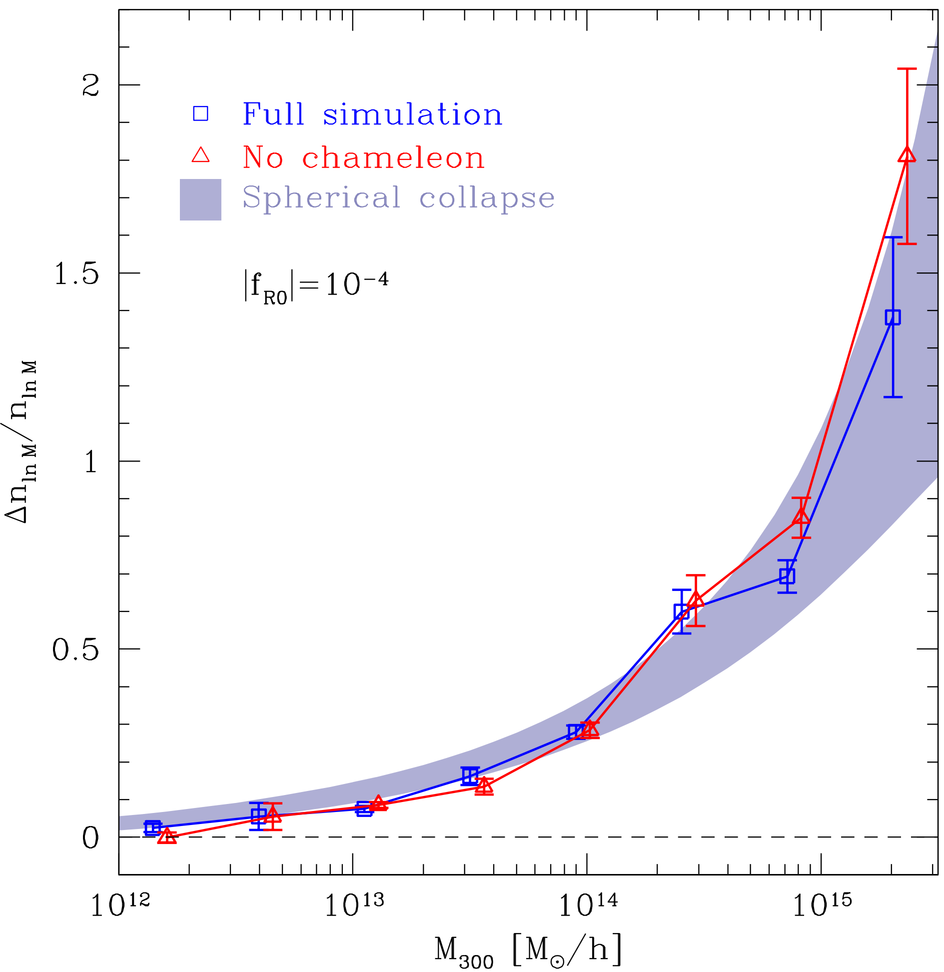

- $|f_{R0}| = 10^{-4}$
- Large enhancement at high masses.
- Full f_R: Less enhancement due to chameleon effect.

Schmidt, Lima, Oyaizu, Hu 2009

$f(R)$ gravity: Halo-mass function

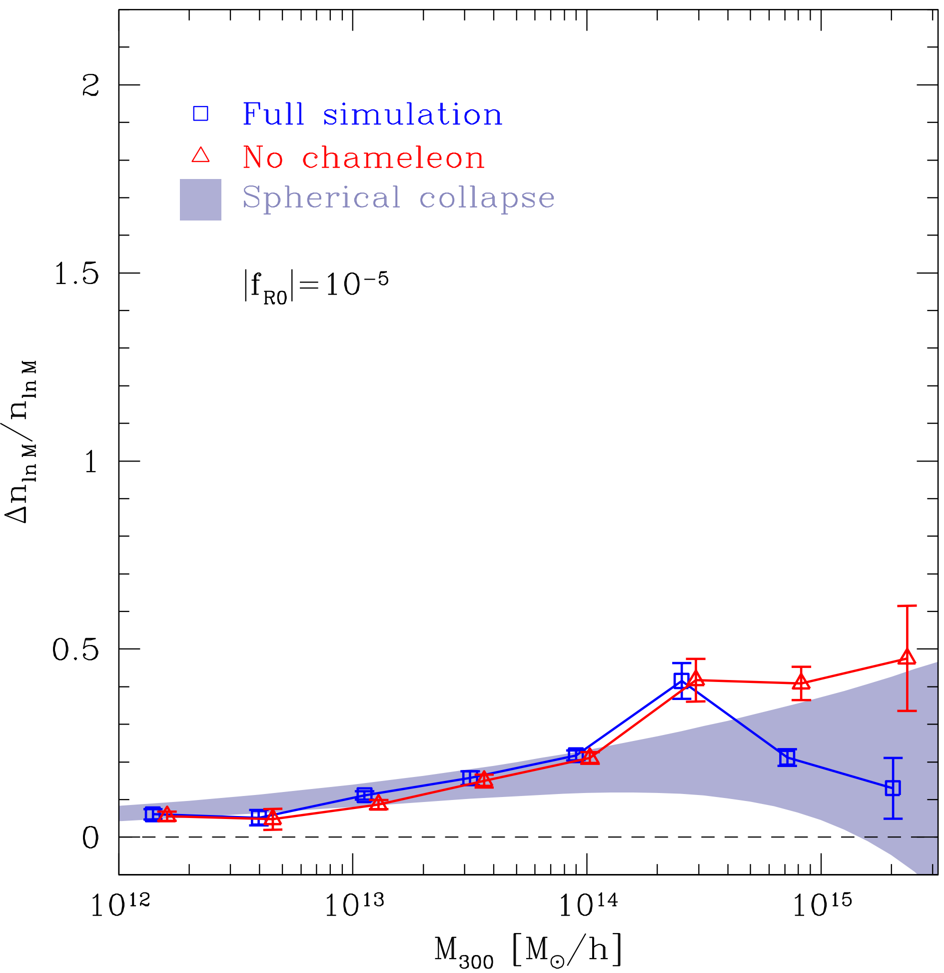

- $|f_{R0}| = 10^{-5}$
- Less relative deviation.
- Enhanced chameleon effect.

Schmidt, Lima, Oyaizu, Hu 2009

Cluster Abundance Prediction

- Abundance described by mass function:

$$\frac{dn(M,z)}{d\ln M} = f(\sigma)\frac{\bar{\rho}_{\rm m}}{M}\frac{d\ln\sigma^{-1}}{d\ln M}\,, \qquad f(\sigma) \propto \exp\left(-1/\sigma^2\right)$$

where

$$\sigma^2(R) = \int \frac{d^3k}{(2\pi)^3}|\tilde{W}(kR)|^2 P_m^L(k,z)\,, \qquad R = (3M/4\pi\bar{\rho}_{\rm m})^{1/3}$$

- Exponential sensitivity to cosmology via $P_m^L(k,z)$, as long as precise measurements of M and z.

Density and Counts: Perfect Case

- Number density in mass bin α:

$$\bar{n}_\alpha(z) = \int_{M_\alpha}^{M_{\alpha+1}} d\ln M \frac{dn(M,z)}{d\ln M}\,,$$

- Number counts in redshift bin i:

$$\bar{N}_{\alpha i} = \int_{z_i}^{z_{i+1}} \underbrace{dz \frac{D_A^2(z)}{H(z)}}_{dV\text{: volume}} \bar{n}_\alpha(z)\,,$$

- For a flat Universe, the comoving angular-diameter distance is simply the radial comoving distance $D_A = \chi$ and

$$\chi(z) = \int_0^z \frac{dz}{H(z)}$$

Number Density: MO Relation

- Number density in observed mass bin α:

$$\bar{n}_\alpha(z) = \int_{M_\alpha^{\rm obs}}^{M_{\alpha+1}^{\rm obs}} d\ln M^{\rm obs} \int d\ln M \frac{dn(M,z)}{d\ln M} \underbrace{P(M^{\rm obs}|M)}_{\text{mass-observable}},$$

where

$$P(M^{\rm obs}|M) = \frac{1}{\sqrt{2\pi\sigma^2_{\ln M}}} \exp\left[\frac{(\ln M^{\rm obs} - \ln M - \ln M_{\rm bias})^2}{2\sigma^2_{\ln M}}\right]$$

- $\ln M_{\rm bias}(z,M)$ and $\sigma^2_{\ln M}(z,M)$: functional forms from simulations, calibration sets, or simply self-calibrated.

Number Counts: Photo-zs

- Number counts in photometric redshift bin i:

$$\bar{N}_{\alpha i} = \int_{z_i^{\rm phot}}^{z_{i+1}^{\rm phot}} dz^{\rm phot} \int dz \frac{D^2(z)}{H(z)} n_\alpha(z) P(z^{\rm phot}|z) \,,$$

where

$$P(z^{\rm phot}|z) = \frac{1}{\sqrt{2\pi\sigma_z^2}} \exp\left[\frac{(z^{\rm phot} - z - z_{\rm bias})^2}{2\sigma_z^2}\right]$$

- $z_{\rm bias}(z, M)$ and $\sigma_z^2(z, M)$: functional forms from simulations, calibration sets, or simply self-calibrated.

Counts and Photo-z Parameters

- z^{bias}: systematic shifts in dN/dz.

  σ_z: random scatter in different bins. Compensating effects.

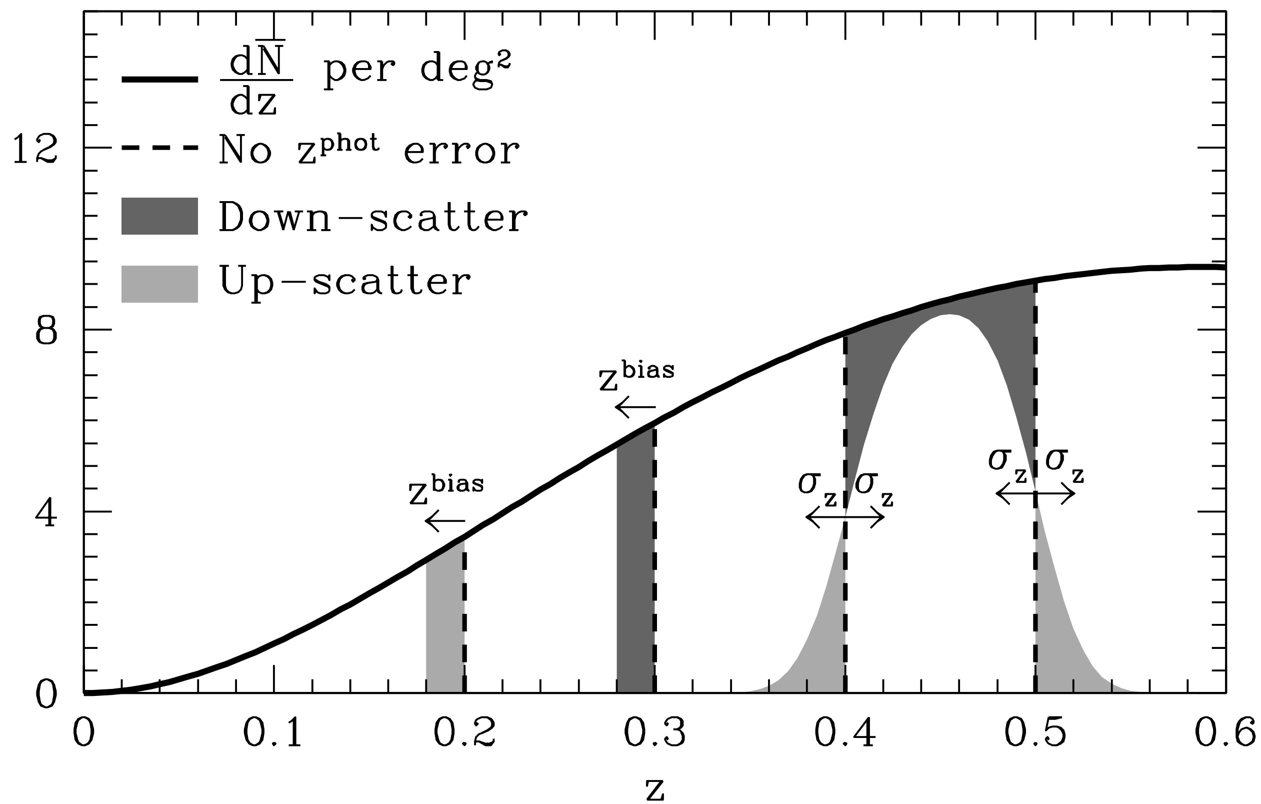

Lima and Hu 2007

Halo and Cluster Finders

- In N-body simulations, one has to identify dark matter halos from the positions (and velocities) of dark matter particles.
- Main two halo-finders: Spherical Overdensity (SO) and Friends-of-Friends (FOF).
- Halo mass-function fits are connected to Halo finder and to halo mass definition.
- E.g. M_{200} is mass contained within R_{200}, the radius where the enclosed cluster overdensity is 200 times the background density, i.e. $\Delta = 1 + \delta_h = 200$
- Methods to identify real clusters even more complicated. Can be based on overdensity of galaxies, colors, weak lensing, x-ray emission and SZ effect of CMB photons.
- Frequently methods fail to detect clusters, and/or identify false clusters. Must characterize those for use in cosmology.

Counts: Completeness and Purity

- Completeness (c): Fraction of correctly detected clusters (halos) from total predicted clusters/halos.
- Purity (p): Fraction of correctly detected clusters from total detected clusters.
- Example: True number of predicted clusters/halos is 100. Finder detects 80 clusters, from which 70 are correct and 10 are spurious. Then $c = 7/10$ and $p = 7/8$.
- Original prediction (100) must be corrected to number that ends up being (correctly or incorrectly) detected (80), i.e multiplied by

$$\frac{8}{10} = \frac{7/10}{7/8} = \frac{c}{p}$$

Rozo et al 2007, Soares-Santos et al. 2010

Counts: Completeness and Purity

- $c(M,z)$ and $p(M_{\rm obs}, z^{\rm phot})$ must be parametrized and included in the counts prediction. Extra functions to be integrated over:

$$
\begin{aligned}
\bar{N}_{\alpha i} &= \int_{z_i^{\rm phot}}^{z_{i+1}^{\rm phot}} dz^{\rm phot} \int dz \frac{D^2(z)}{H(z)} P(z^{\rm phot}|z) \\
&\times \int_{M_\alpha^{\rm obs}}^{M_{\alpha+1}^{\rm obs}} d\ln M^{\rm obs} \int d\ln M \, P(M^{\rm obs}|M) \\
&\times \frac{dn(M,z)}{d\ln M} \times \frac{c(M,z)}{p(M_{\rm obs}, z^{\rm phot})}
\end{aligned}
$$

- Else, restrict analysis to region where $c \approx p \approx 1$ (higher M, lower z), but lose statistics...

Cluster Bias

- Spherical collapse: fraction of matter regions which have collapsed to form halos depends on the matter density field.
- Overdense regions have higher probability of forming halos and time evolution makes them even more likely to cross the collapse threshold $\rightarrow$ cosmic capitalism from gravity.
- The large scale density field develops local enhanced peaks $\rightarrow$ effectively lowers collapse threshold δ_c.
- Discrete number density of halos becomes a biased tracer of the continuous matter density field.
- Halos trace matter field, but bias accounts for the fact that they correspond to a special population, whose average properties are different from those of the average density field.
- Bias increases with halo mass, as these objects are rarer and even more unique.

Cluster Bias

- Quantify effects by adding a background contribution $\delta^{\rm b}$ to the peak matter overdensity $\delta^{\rm p}$.
- Total overdensity given by $\delta = \delta^{\rm p} + \delta^{\rm b}$.

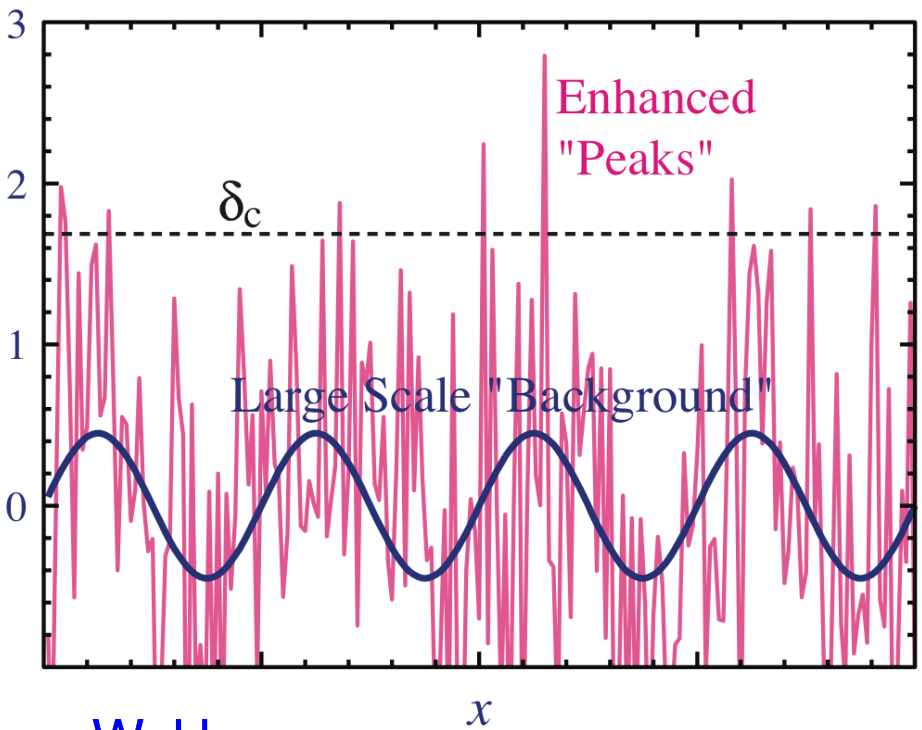

W. Hu

- Mathematically equivalent to keeping $\delta = \delta^{\rm p}$ and lowering the threshold collapse overdensity by the background contribution

$$\delta_c^{\rm p} = \delta_c - \delta^{\rm b}$$

- Peak-Background split

Cluster Bias

- Mass-function found actually provides matter number density in halo regions

$$n_{\rm m} = \frac{dn}{d\ln M} = f(\sigma, \delta_c)\frac{\bar{\rho}_{\rm m}}{M}\frac{d\ln\sigma^{-1}}{d\ln M}$$

- Halo number density $n_{\rm h}$ obtained by changing

$$\begin{aligned} \delta_c \rightarrow \delta_c^{\rm p} &= \delta_c - \delta^{\rm b} \\ \nu &= \delta_c^{\rm p}/\sigma \end{aligned}$$

- Express $n_{\rm h}$ in terms of $n_{\rm m}$ by expanding to first order

$$\begin{aligned} n_{\rm h} &= f(\sigma, \delta_c^{\rm p})\frac{\bar{\rho}_{\rm m}}{M}\frac{d\ln\sigma^{-1}}{d\ln M} \\ &= \left[f(\sigma, \delta_c) - \frac{df}{d\delta_c^{\rm p}}\delta^{\rm b}\right]\frac{\bar{\rho}_{\rm m}}{M}\frac{d\ln\sigma^{-1}}{d\ln M} \end{aligned}$$

Cluster Bias

$$
\begin{aligned}
n_{\rm h} &= \left[f(\sigma,\delta_c) - \frac{df}{d\delta_c^{\rm p}}\delta^{\rm b} \right] \frac{\bar\rho_{\rm m}}{M} \frac{d\ln\sigma^{-1}}{d\ln M} \\
&= \underbrace{f(\sigma,\delta_c)\frac{\bar\rho_{\rm m}}{M}\frac{d\ln\sigma^{-1}}{d\ln M}}_{n_m} - \underbrace{\frac{1}{f}\frac{df}{d\nu}}_{d\ln f/d\nu} \underbrace{\frac{d\nu}{d\delta_c^{\rm p}}}_{1/\sigma} \delta^{\rm b} \underbrace{f\frac{\bar\rho_{\rm m}}{M}\frac{d\ln\sigma^{-1}}{d\ln M}}_{n_m} \\
&= n_{\rm m}\left[1 - \frac{1}{\sigma}\frac{d\ln f}{d\nu}\delta^{\rm b} \right]
\end{aligned}
$$

- Since $\langle\delta^{\rm b}\rangle = 0$ we have $\bar n_h = \bar n_m$.

Cluster Bias

- In an unbiased density field, an increase of local density by $\delta^{\rm b}$ would turn $n_{\rm m} \to n_{\rm m}(1+\delta^{\rm b})$, i.e. induce a change of $\Delta_{\rm m} = n_{\rm m}\delta^{\rm b}$.
- However, actual change in $n_{\rm h}$ is $\Delta_{\rm h} = -n_{\rm m}\delta^{\rm b}(d\ln f/d\nu)/\sigma$, i.e. it is enhanced by

$$E_{\rm hm} = \frac{\Delta_{\rm h}}{\Delta_{\rm m}} = -\frac{1}{\sigma}\frac{d\ln f}{d\nu}$$

- Therefore, spatial fluctuations of the halo number density $\delta_{\rm h} = \delta n_{\rm h}/n_{\rm h}$ are those of the matter $\delta_{\rm m} = \delta n_{\rm m}/n_{\rm m}$ plus those from the enhancement of halos relative to matter

$$\delta_h = \delta_{\rm m} + \delta_{\rm m}E_{\rm hm} = \delta_{\rm m}\left(1 - \frac{1}{\sigma}\frac{d\ln f}{d\nu}\right)$$

- Halo bias defined via $b \equiv \delta_{\rm h}/\delta_{\rm m}$.

Cluster Bias

- Halo bias defined via $b \equiv \delta_{\rm h}/\delta_{\rm m}$, can be computed for any mass-function defined in terms of δ_c by

$$b(z, M) \quad = \quad 1 - \frac{1}{\sigma}\frac{d\ln f}{d\nu}$$

- For the PS mass-function $f(\nu) \propto \nu \exp(-\nu^2/2)$, so

$$b(z, M) \quad = \quad 1 + \frac{\nu^2 - 1}{\delta_c}$$

Press Schechter

- For the ST mass-function

$$b(z, M) \quad = \quad 1 + \frac{a^2\nu^2 - 1}{\delta_c} + \frac{2p}{\delta_c[1 + (a\nu^2)^p]}$$

Sheth Tormen

Cluster Bias

- Spherical collapse: approximation for the halo mass-function,
- Peak-background split: approximation for the halo bias.
- As for the mass-function, modern approach for precision cosmology is to fit $b(z, M)$ from N-body simulations. For example, as done for SO halos by Tinker et al. 2010

$$b(z, M) \;=\; 1 - A\frac{\nu^a}{\nu^a + \delta_c^a} + B\nu^b + C\nu^c \qquad \text{Tinker}$$

- Average bias $b_{i,\alpha}$ in bin i, α

$$b_{i,\alpha} = b(z_i, M_\alpha) = \frac{1}{\bar{N}_{i,\alpha}} \int_{z_i}^{z_{i+1}} dz \frac{D_A^2(z)}{H(z)} \int_{M_\alpha}^{M_{\alpha+1}} d\ln M \frac{dn}{d\ln M} b(z, M)$$

Cluster Covariance

- Observed cluster counts fluctuate in space because
  - The discrete counting process: Poisson Variance$= \delta_{ij}\bar{N}_i$
  - They trace large-scale structure: Sample Covariance$= S_{ij}$.
- Observed number density in bin i (for both redshift and mass):

$$n_i(\mathbf{x}) = \bar{n}_i[1 + b_i\delta(\mathbf{x})]$$

- Number counts posses Sample Covariance S_{ij}

$$S_{ij} \equiv \langle (N_i - \bar{N}_i)(N_j - \bar{N}_j)\rangle$$

- Write N_i in terms of window $W_i(\mathbf{x})$ specifying bin i

$$N_i = \int d^3x W_i(\mathbf{x}) n_i(\mathbf{x}), \qquad \bar{N}_i = \int d^3x W_i(\mathbf{x})\bar{n}_i \approx V_i\bar{n}_i$$

Cluster Covariance

$$N_i = \int d^3x W_i(\mathbf{x}) n_i(\mathbf{x}), \qquad \bar{N}_i = \int d^3x W_i(\mathbf{x}) \bar{n}_i \approx V_i \bar{n}_i$$

so that

$$\begin{aligned} N_i - \bar{N}_i &= \int d^3x W_i(\mathbf{x}) \left[n_i(\mathbf{x}) - \bar{n}_i \right] \\ &= \bar{n}_i b_i \int d^3x W_i(\mathbf{x}) \delta(\mathbf{x}) \end{aligned}$$

- Sample covariance S_{ij} becomes

$$\begin{aligned} S_{ij} &= \langle b_i b_j \bar{n}_i \bar{n}_j \int d^3x W_i^*(\mathbf{x}) \int \frac{d^3k}{(2\pi)^3} \delta^*(\mathbf{k}) e^{-i\mathbf{k}\cdot\mathbf{x}} \\ &\qquad \int d^3x' W_j(\mathbf{x}') \int \frac{d^3k'}{(2\pi)^3} \delta(\mathbf{k}') e^{i\mathbf{k}'\cdot\mathbf{x}'} \rangle \end{aligned}$$

Cluster Covariance

$$
\begin{aligned}
S_{ij} &= \langle b_i b_j \bar{n}_i \bar{n}_j \int d^3x W_i^*(\mathbf{x}) \int \frac{d^3k}{(2\pi)^3} \delta^*(\mathbf{k}) e^{-i\mathbf{k}\cdot\mathbf{x}} \\
&\quad \times \int d^3x' W_j(\mathbf{x}') \int \frac{d^3k'}{(2\pi)^3} \delta(\mathbf{k}') e^{i\mathbf{k}'\cdot\mathbf{x}'} \rangle \\
&= b_i b_j \bar{n}_i \bar{n}_j \int d^3x W_i^*(\mathbf{x}) \int d^3x' W_j(\mathbf{x}') \\
&\quad \times \int \frac{d^3k}{(2\pi)^3} \int \frac{d^3k'}{(2\pi)^3} \underbrace{\langle \delta(\mathbf{k}) \delta^*(\mathbf{k}') \rangle}_{(2\pi)^3 \delta^3(\mathbf{k}-\mathbf{k}') P(k)} e^{-i\mathbf{k}\cdot\mathbf{x}} e^{i\mathbf{k}'\cdot\mathbf{x}'} \\
&= b_i b_j \bar{N}_i \bar{N}_j \int \frac{d^3k}{(2\pi)^3} P(k) \underbrace{\int \frac{d^3x}{V_i} W_i^*(\mathbf{x}) e^{-i\mathbf{k}\cdot\mathbf{x}}}_{W_i^*(\mathbf{k})} \underbrace{\int \frac{d^3x'}{V_j} W_j(\mathbf{x}') e^{i\mathbf{k}\cdot\mathbf{x}'}}_{W_j(\mathbf{k})}
\end{aligned}
$$

- We used $\bar{N}_i \approx n_i V_i$

Cluster Covariance

$$S_{ij} \quad = \quad b_i b_j \bar{N}_i \bar{N}_j \int \frac{d^3k}{(2\pi)^3} P(k) W_i^*(\mathbf{k}) W_j(\mathbf{k})$$

- $W_i(\mathbf{k})$ is the volume-weighted Fourier Transform of the window.
- For a pill-box window (in the small angle approximation) at redshift z_i and radial distance r_i, with angular extent θ (and solid angle $\Delta\Omega = \pi\theta^2$), and radial extent δr_i, the window is given by

$$W_i(\mathbf{k}) = 2e^{ik_{\parallel} r_i} \frac{\sin(k_{\parallel}\delta r_i/2)}{k_{\parallel}\delta r_i/2} \frac{J_1(k_{\perp} r_i \theta)}{k_{\perp} r_i \theta}$$

Hu and Kravtsov 2003

- Finally, total covariance

$$C_{ij} = \delta_{ij}\bar{N}_i + S_{ij}$$

Cluster Likelihood

- Likelihood of drawing set of cluster counts $\mathbf{N} = (N_1, N_2, ..., N_b)$ given a cosmology-dependent model for $\bar{\mathbf{N}}$ and $\mathbf{S}$: $L(\mathbf{N}|\bar{\mathbf{N}}, \mathbf{S})$.
- Accounts for both Poisson and Sample Variance:

$$L(\mathbf{N}|\bar{\mathbf{N}}, \mathbf{S}) = \int d^b \bar{N}' \left[\prod_{i=1}^{b} \underbrace{P(N_i|\bar{N}_i')}_{\text{Poisson}} \right] \underbrace{G(\bar{\mathbf{N}}'|\bar{\mathbf{N}}, \mathbf{S})}_{\text{Gaussian}}$$

For $N_i \gg 1$, Poisson $\rightarrow$ Gaussian. After convolution, get:

$$L(\mathbf{N}|\bar{\mathbf{N}}, \mathbf{S}) \approx G(\mathbf{N}|\bar{\mathbf{N}}, \mathbf{C}) \quad \text{Gaussian}$$

with total covariance

$$C_{ij} = \delta_{ij} \bar{N}_i + S_{ij}$$

Cluster Forecasts: Fisher Matrix

- Fisher Matrix: Allows projections of likelihood analyses.
- Model parameters: p_α, i.e. $\bar{N}_i(p_\alpha)$, $S_{ij}(p_\alpha)$.
- Defining $_{,\alpha} = \partial/\partial p_\alpha$, Fisher is:

$$
\begin{aligned}
F_{\alpha\beta} &= -\langle \frac{\partial \ln L}{\partial p_\alpha \partial p_\beta} \rangle \\
&= \bar{N}_{,\alpha} \mathbf{C}^{-1} \bar{N}_{,\beta} + \frac{1}{2} \mathrm{Tr}[\mathbf{S}^{-1} \mathbf{S}_{,\alpha} \mathbf{S}^{-1} \mathbf{S}_{,\beta}]
\end{aligned}
$$

- Sample Variance: Noise in the first term, Signal in the second.

Cluster Forecasts: Dark Energy

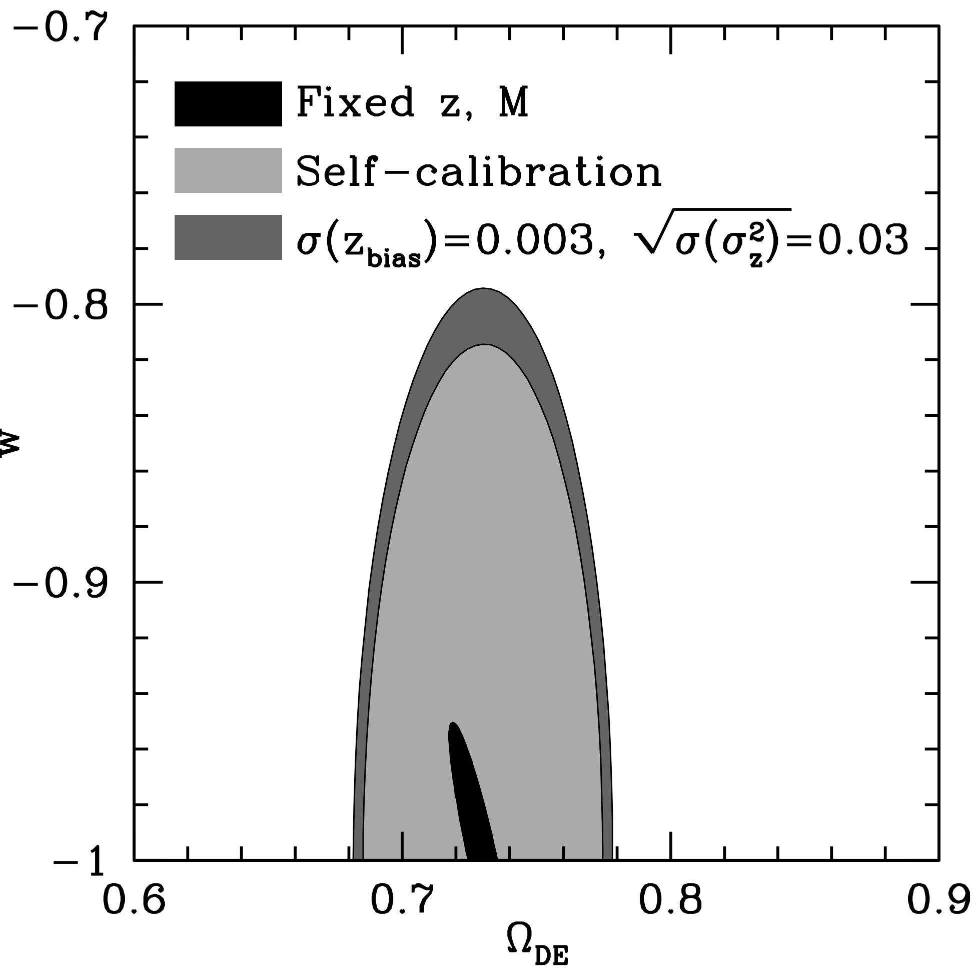

Lima and Hu 2007

- Fisher matrix constraints on Dark Energy: $\Omega_{\rm DE}$ e w.
- High precision with perfect M and z.
- No precision calibrating M with abundance only.
- Precision restored with self-calibration (abundance + clustering).
- Uncertainty on photo-z errors for 10% degradation in w.

Cluster Forecasts: Dark Energy

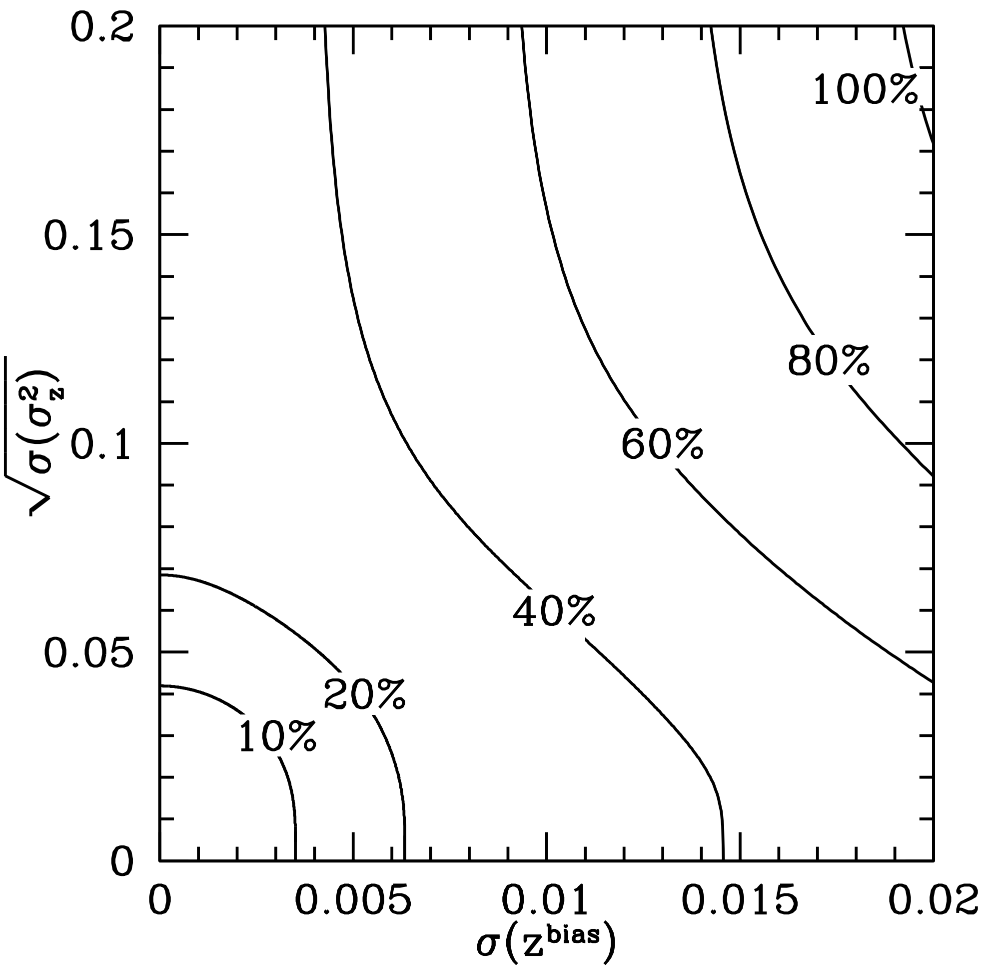

Lima and Hu 2007

- Uncertainty in $z_{\rm bias}$ and σ_z^2
- Contours of constant degradation in w relative to case of perfect redshifts.

$$\sigma(z^{\rm bias}) = \sigma_z\sqrt{\frac{1}{N}}$$

$$\sigma(\sigma_z^2) = \sigma_z^2\sqrt{\frac{2}{N}}$$

- Requirement on N: size of spectroscopic calibrating set.

Cluster Constraints: MCMC

- Actual constrains from full Likelihood analysis.
- MCMC: Random walk in parameter space.
  - Start at initial point in parameter space p_α^i and compute L^i.
  - Generate random step to p_α^{i+1} and compute L_{i+1}.
  - Define $\alpha = L_{i+1}/L_i$.
  - If $\alpha > 1$, take step, add new point to chain.
  - Else, generate random number $r \in [0, 1]$.
    - If $\alpha > r$, take step, add new point to chain.
    - Else, do not take step, add old point to chain.
  - Repeat...
- Bayes' Theorem: Chain is fair sample of parameters' posterior.

Cluster MCMC: BCC Halos Results

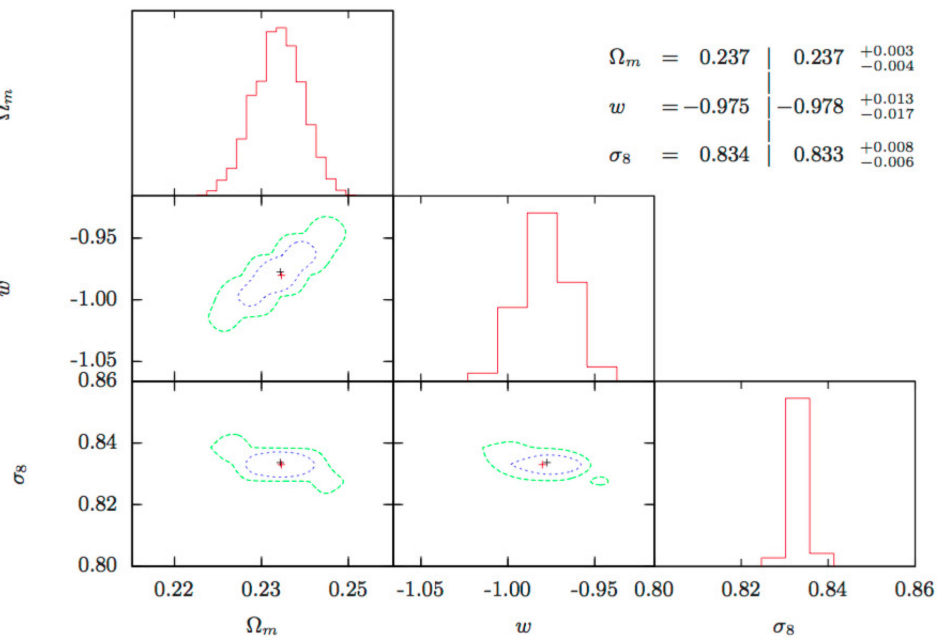

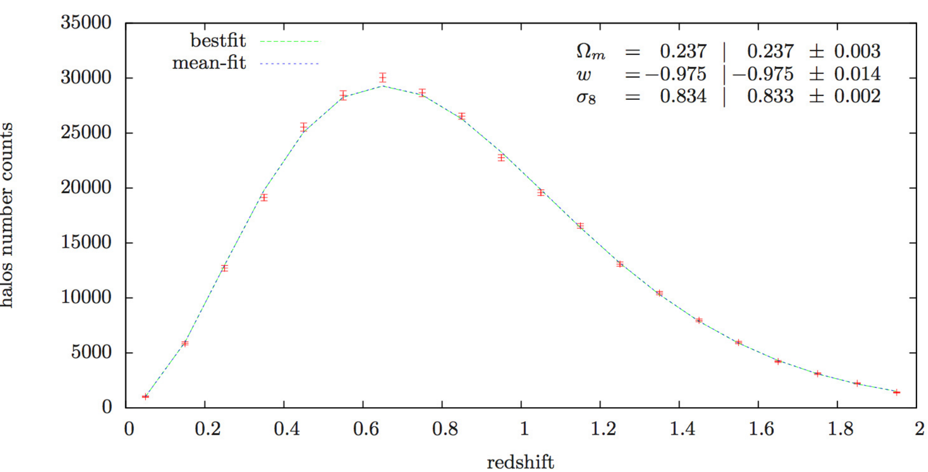

- BCC halos, not clusters yet.
- Consistent with Fisher prediction and BCC cosmology.
- More parameters: degeneracies hard to break with clusters alone, even with more mass bins.
- Explore priors.
- Use WZAP cluster catalog with real-life details.

Aguena and Lima

Cluster MCMC: BCC Halos Results

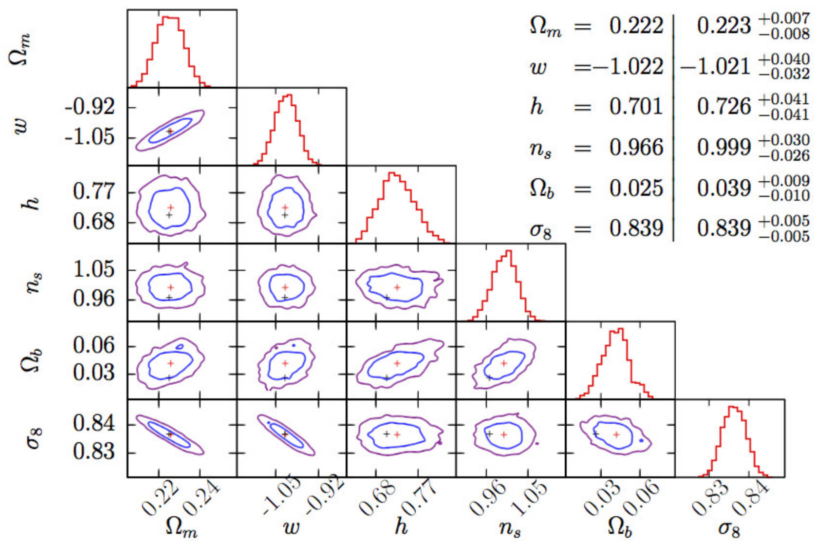

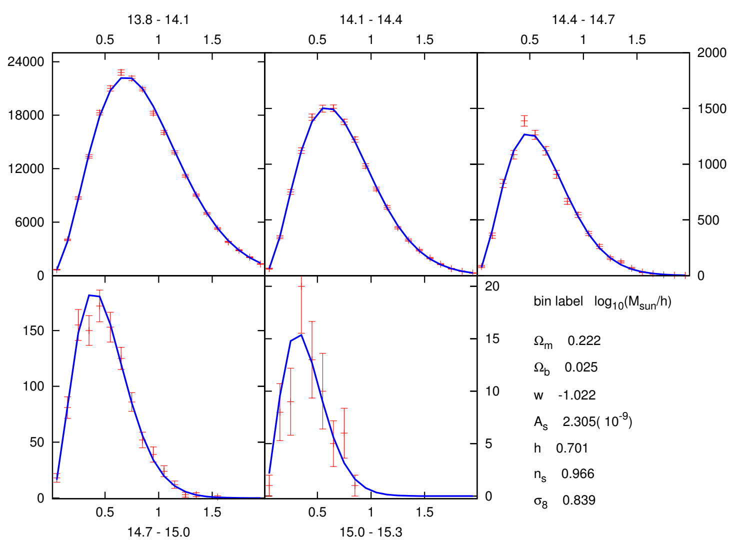

- BCC halos, not clusters yet.
- Consistent with Fisher prediction and BCC cosmology.
- More parameters: degeneracies hard to break with clusters alone, even with more mass bins.
- Explore priors.
- Use WZAP cluster catalog with real-life details.

Aguena and Lima